

Article

Fabrication of pH-Responsive PDPAEMA Thin Film Using a One-Step Environmentally Friendly Plasma Enhanced Chemical Vapor Deposition

Mehmet Gürsoy 

Chemical Engineering Department, Konya Technical University, 42030 Konya, Turkey; mgursoy@ktun.edu.tr; Tel.: +90-3322231972

Abstract: In recent years, there has been growing interest in pH-responsive polymers. Polymers with ionizable tertiary amine groups, which have the potential to be used in many critical application areas due to their pKa values, have an important place in pH-responsive polymers. In this study, poly(2-Diisopropyl aminoethyl methacrylate) (PDPAEMA) thin films were coated on various substrates such as glass, fabric, and silicon wafer using a one-step environmentally friendly plasma enhanced chemical vapor deposition (PECVD) method. The effects of typical PECVD plasma processing parameters such as substrate temperature, plasma power, and reactor pressure on the deposition rate were studied. The highest deposition rate was obtained at a substrate temperature of 40 °C, a reactor pressure of 300 mtorr, and a plasma power of 60 W. The apparent activation energy was found to be 17.56 kJ/mol. Based on the results of this study, uniform film thickness and surface roughness were observed in a large area. The PDPAEMA thin film was exposed to successive acid/base cycles. The results showed that the pH sensitivity of the thin film produced by the PECVD method is permanent and reversible.

Keywords: polymer coating; pH-responsive; PDPAEMA; thin film; PECVD; functional coating



Citation: Gürsoy, M. Fabrication of pH-Responsive PDPAEMA Thin Film Using a One-Step Environmentally Friendly Plasma Enhanced Chemical Vapor Deposition. *Coatings* **2024**, *14*, 347. <https://doi.org/10.3390/coatings14030347>

Academic Editor: Andriy Voronov

Received: 26 February 2024

Revised: 11 March 2024

Accepted: 13 March 2024

Published: 14 March 2024



Copyright: © 2024 by the author. Licensee MDPI, Basel, Switzerland. This article is an open access article distributed under the terms and conditions of the Creative Commons Attribution (CC BY) license (<https://creativecommons.org/licenses/by/4.0/>).

1. Introduction

Stimuli responsive polymers have significant potential for a wide range of engineering, scientific, and industrial processes, because of their unique switchable properties. The physicochemical properties of stimuli responsive polymers change as a result of various physical and/or chemical stimuli in their environment [1–3]. When the stimulus responsible for the change returns to its initial state, the changed physicochemical properties return to their initial state. pH, temperature, light, and magnetic field are among the most common stimuli in the literature [4–7]. Considering the role of solvents in chemical and biochemical processes, it can be suggested that pH is a highly effective stimulus. A slight increase or decrease in the pH value of the medium can cause changes in the chain structure, solubility, volume, wettability, and similar structural properties of pH-responsive materials [8]. The reason for these changes is the ionizable functional groups in the structures of the responsive polymers that have the ability to accept or donate protons depending on the pH of the environment [9]. Depending on whether these groups are weakly acidic or weakly basic, pH-responsive polymers can be generally divided into two main groups: polyacids and polybases [10]. Pendant acid groups such as carboxylic acids in polyacids and basic groups such as amines in polybases are ionized depending on the pH of the medium. If the pH of the medium is lower than the dissociation constant (pKa) of the polymers, then polyacids are deprotonated and shrink, while polybases are protonated and expand. In this case, polyacids and polybases exhibit hydrophobic and hydrophilic properties, respectively [11].

One of the most important potential application areas of pH-responsive polymers is drugs used in the diagnosis/treatment of cancer. Since cancer cells are much more dependent on aerobic glycolysis for ATP than healthy cells, the extracellular environment of tumor cells is

more acidic [12]. It is known that the pH value around tumors is between 6.2–6.8 [13]. The pKa values of methacrylate polymers with tertiary amine groups are mostly in this range [14]. That is why these polymers have an important place among pH-responsive polymers. There is an increasing interest in the fabrication of this class of polymers such as poly(2-diethylaminoethyl methacrylate) (PDEAEMA), poly(2-dimethylaminoethyl methacrylate) (PDMAEMA), and poly(2-diisopropylaminoethyl methacrylate) (PDPAEMA) [15–17].

The fabrication methods of polymers can be categorized under two main classes: wet and dry methods. Sol-gel, dip-coating, atom transfer radical polymerization (ATRP), and reversible addition-fragmentation chain-transfer (RAFT) can be given as examples of wet processes [18–21]. These methods are relatively easy to implement and generally do not require expensive or special equipment. However, the solvents used in wet processes can cause damage to fragile substrates. Strong solvent tension forces prevent homogeneous and conformal polymer formation on the surface of complex geometry substrates with porous or corrugated parts. Furthermore, the solutions used in wet methods pose a threat to both the environment and the health of all organisms. Hence, additional processes are required to remove the solutions, resulting in higher energy consumption and cost. On the other hand, dry methods, as its name implies, eliminate all solvent-related issues including the use of hazardous solvents, solvent disposal steps, and multiple washing/rinsing cycles, which make dry methods such as chemical vapor deposition (CVD) environmentally friendly. Therefore, environmentally friendly plasma enhanced CVD (PECVD) can be considered as an effective technique for the fabrication of polymers in a one-step method and at low temperature. In addition, PECVD has significant advantages such as real-time film thickness measurement and the ability to be easily employed into large-scale production [22,23].

The primary aim of this study is to fabricate pH-responsive PDPAEMA thin film using a rapid, one-step, and environmentally friendly method. In this study, the versatile PECVD method was selected for the fabrication of PDPAEMA thin film, due to the aforementioned advantages. The effects of some important PECVD process parameters such as reactor pressure, substrate temperature, and plasma power on the deposition rate were investigated. The surface properties of PDPAEMA thin film were investigated by using a series of instruments including Fourier-transform infrared spectroscope (FTIR), X-ray photoelectron spectroscope (XPS), atomic force microscope (AFM), scanning electron microscope (SEM), profilometer, UV/Vis spectrophotometer, and contact angle goniometer. The PECVD parameters for the highest PDPAEMA thin film deposition rate were determined and the apparent activation energy was calculated. Furthermore, the uniformities of film thickness and surface roughness of the PDPAEMA thin film in large areas were investigated.

2. Materials and Methods

2.1. Materials

Silicon wafer (100, p-type), glass slide (ISOLAB Laborgeräte GmbH, Wertheim, Germany), and fabric (40 g, polypropylene spunbond non-woven, Rota Teknik Tekstil, İstanbul, Türkiye) were used as substrates. The monomer DPAEMA (97%, Sigma-Aldrich, Steinheim, Germany) was used as received without any further purification and modification. Ultrapure nitrogen (99.999%) was used as a carrier gas to transport the monomer into the vacuum reactor.

2.2. Thin Film Synthesis by PECVD

The polymerization was carried out under vacuum in a custom-designed stainless-steel reactor with a cylindrical geometry having a height of 10 cm and an outer diameter of 16 cm. A more detailed description of the PECVD setup used in this study is given elsewhere [24]. The schematic drawing of the PECVD setup is shown in Figure 1a. The required vacuum in the reactor was achieved by a rotary vane vacuum pump. The pressure inside the reactor was measured with the help of a capacitance type barometer. The pressure was controlled by a butterfly throttling valve (MKS instruments, Andover, MA, USA) placed

between the pump and the reactor. In order to keep the reactor pressure constant at the desired value during the experiments, a proportional-internal-derivative (PID) control unit connected to both the barometer and the butterfly throttling valve was used. The monomer was put in a stainless-steel jar and clamped to the manifold pipeline to feed in the reactor using nitrogen as the carrier gas. The monomer jar and manifold line were wrapped with heating tapes controlled by a PID temperature heater. The jar and line were heated to 70 and 80 °C, respectively. An on-off and a needle valve (Swagelok, Solon, OH, USA) on the line ensured that monomer vapor was fed into the vacuum reactor at the desired flow rate. The substrates were placed on the reactor bottom with a heat exchanger on the backside. The heat exchanger was connected to a recirculating chiller to maintain the substrate temperature at the desired temperature during the experiments. The reactor lid was quartz, which allowed for real-time thickness monitoring using a laser interferometer. A more detailed description of the laser interferometer is given elsewhere [25]. The activation energy required to initiate polymerization was provided by plasma discharge generated inside the reactor. To generate the plasma discharge, a copper antenna connected to a plasma power generator (13.56 MHz) was placed on the reactor lid. A matching box was placed between the copper antenna and the plasma power supply to ensure stable plasma generation inside the vacuum reactor without back reflection. The PECVD parameters studied are given in Table 1. The plasma polymerization reaction of DPAEMA in PECVD is shown in Figure 1b.

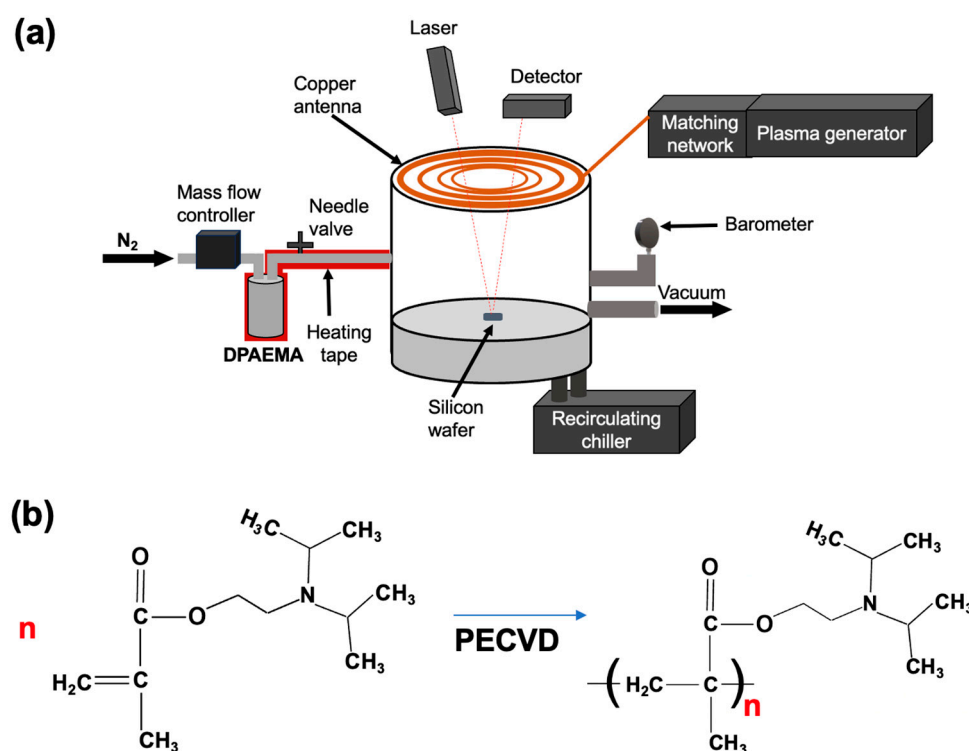


Figure 1. (a) The schematic drawing of the PECVD system, (b) The reaction scheme of DPAEMA in PECVD. Red *n* is the number of repeating monomer units.

Table 1. PECVD parameters for PDPAEMA deposition.

Parameter	Value
Substrate temperature (°C)	10, 20, 30, and 40
Reactor pressure (mtorr)	100, 300, and 500
Plasma power (W)	20, 40, 60, and 80

2.3. Characterizations

The thicknesses of the thin films deposited on silicon wafers were measured by both in-situ (laser interferometer) and ex-situ (AEP 500LS profilometer, Santa Clara, CA, USA) methods. The deposition rates of the films were calculated by dividing the thickness of the films by the deposition times. The chemical structure of the PDPAEMA thin film was revealed by FTIR and XPS analyses. FTIR analysis of the PDPAEMA thin film and the DPAEMA monomer were performed using a FTIR spectrometer (Bruker Vertex 70, Ettlingen, Germany) at a resolution of 4 cm^{-1} with 32 scans. For FTIR analysis, as-deposited thin film on the glass slide was scraped off with a flat blade scalpel. XPS analysis of the PDPAEMA thin film was performed with an Al source ($h\nu = 1486.68\text{ eV}$) using a Thermo Scientific K-Alpha XPS (Thermo Fisher Scientific, Loughborough, UK). The XPS instrument was calibrated to the reference peak positions of Au 4f7/2 (84.00 eV), Ag 3d5/2 (368.26 eV), and Cu 2p3/2 (932.67 eV). The survey spectrum was operated with a pass energy of 200 eV, an energy step size of 1 eV, and a dwell time of 50 s. The high-resolution mode was operated with a pass energy of 30 eV, an energy step size of 0.1 eV, and a dwell time of 50 s. Spectral deconvolution was performed using Advantage Software v5.9916 without any restrictions on the spectral position. Quantification of the XPS spectrum was performed by normalizing the calculated peak area using the relevant Scofield relative sensitivity factors. SEM (EVO LS-10 Zeiss, Carl Zeiss, Oberkochen, Germany) was used to investigate the morphologies of the fabric before and after PDPAEMA thin film coating. Before SEM analysis, the samples were placed on sample holders and coated with a gold layer of approximately 5 nm using a sputter coater (Cressington Scientific Instruments Ltd., Watford, UK). The optical transmittance of the PDPAEMA coated glass was measured in the wavelength range from 300 to 800 nm using a UV/Vis spectrophotometer (Shimadzu UV-1800, Shimadzu Inc., Kyoto, Japan) with a spectral resolution of 1 nm. Contact angle measurement of the PDPAEMA coated substrate was performed using a contact angle goniometer (OCA 50, Data Physics Instruments GmbH, Filderstadt, Germany). The surface roughness of the PDPAEMA thin film coated silicon wafer in a dimension of $5\text{ }\mu\text{m} \times 5\text{ }\mu\text{m}$ was scanned using AFM (NT-MDT, Ntegra Solaris, Moscow, Russia) in semi-contact mode.

3. Results and Discussion

3.1. Deposition Rates

Deposition rates of polymeric thin films were calculated from in-situ film thicknesses measured by an interferometry system during the polymerization. In the thickness estimation by interferometer, the refractive index of the polymer film is assumed to be constant and the change in the film thickness per fringe is calculated based on Frensel's equation and Snell's law (Equation (1)) [26].

$$\frac{d}{\text{fringe}} = \frac{\lambda}{2\eta_{\text{polymer}}} \quad (1)$$

where d , λ , and η represent the estimated thickness value, the wavelength of the laser used in the interferometer system, and the refractive index of the polymer, respectively. A laser with a wavelength of 633 nm was used and assuming the refractive index of the polymeric thin film to be 1.5, each d/fringe value in Equation (1) was found to be equal to 211 nm. After the depositions were completed, the accuracy of the measured interferometric thickness values was checked by an ex-situ profilometer. It was observed that the thickness values measured by both measurement methods were in perfect agreement. The deposition rates of thin films produced at different plasma power, substrate temperature, and reactor pressure are given in Figure 2.

At the same pressure and substrate temperature, when the plasma power increased from 20 to 60 W, the deposition rates of the films increased. This observation can be

explained by the Yasuda equation (Equation (2)) used to describe the plasma power per unit of gas molecules in plasma polymerization [27].

$$\text{MJ/Kg} = (W/\text{FM}) \times 1340 \quad (2)$$

where W , F , and M represent the applied plasma power (watt), the flow rate of the monomer (sccm), and the molecular weight of the monomer (g/mol), respectively. According to the Yasuda equation, as the applied plasma power under constant conditions increases, the energy input per molecule increases. Therefore, it is expected that increasing plasma power increases the deposition rate. However, as the plasma power increased from 60 to 80 W, a decrease in deposition rates was observed. It is known that in plasma polymerization studies, after a certain level of plasma power, a further increase in plasma power may cause ablation of the deposited films from the surface [28,29]. This could be the reason why the deposition rate decreased with increasing the plasma power from 60 to 80 W.

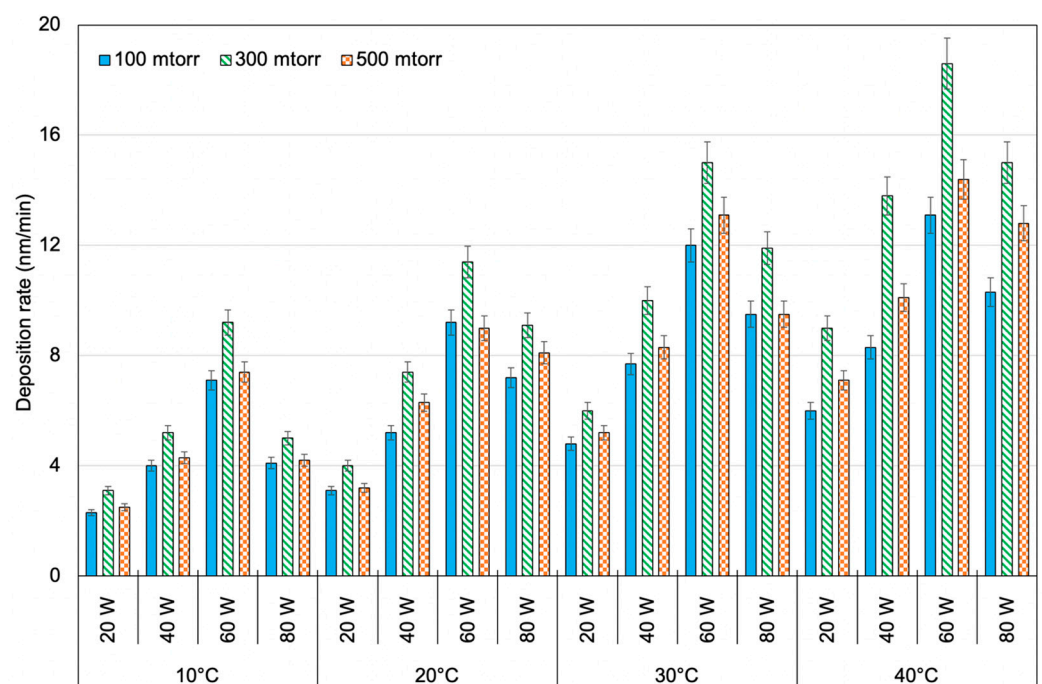


Figure 2. Deposition rates of PDPAEMA thin films deposited at different PECVD parameters.

Reactor pressure is another important CVD parameter, which plays a significant role in the deposition rates [30]. As can be seen in Figure 2, higher deposition rates are obtained when the pressure increases from 100 to 300 mtorr. This can be attributed to the fact that as the pressure increases, the monomer vapor remains in the reactor for a longer time. The increase in the retention time may have increased the number of molecules remaining in the reactor per unit time and consequently the number of molecules adsorbed on the surface may have increased [31]. However, as the pressure was further increased to 500 mtorr, a decrease in the deposition rates was observed. This observed change in the deposition mechanism can be attributed to two possible reasons. The first one is that the further increase in the retention time of the monomer may have caused an increase in the rate of termination. The other possible reason is that the reduction in mean free path may have initiated some gas reactions [32]. The highest deposition rate was found to be 18.6 nm/min at a substrate temperature of 40 °C, a reactor pressure of 300 mtorr, and a plasma power of 60 W. A typical PECVD polymerization process consists of several chemical and physical phenomena. First, monomer vapor is fed into the reactor and then gas diffusion takes place through the boundary layer. As a result of the contact of the gas with the substrate surface, deposition occurs on the substrate surface. Meanwhile,

volatile components are removed from the surface. The slowest process step determines the deposition rate in the CVD process. The most known rate-limiting steps are adsorption (mass transfer) and surface reactions [33]. In this study, the deposition rate increased with increasing substrate temperature when all other PECVD parameters were kept constant. This result indicates that the rate-limiting step in PDPAEMA thin film synthesis is surface reactions. In order to obtain more detailed findings on the deposition kinetic, the apparent activation energy of PDPAEMA thin film deposited at the highest deposition rate was calculated. In the CVD polymerization process, the conversion rate of monomer to polymer is very low [34,35]. That is why it can be assumed that the concentration of monomer in the reactor does not change. Since the monomer vapor concentration is too large to limit the deposition kinetics, the relationship between PECVD parameters and deposition rate can be simplified. Because the plasma power per molecule is also constant, it can be assumed that the deposition rate depends mainly on the substrate temperature. Based on this assumption, the deposition rate as a function of the substrate temperature can be plotted in an Arrhenius form (Equation (3)).

$$\ln k = -\frac{E_a}{RT} + \ln A \quad (3)$$

where k is the reaction rate constant, E_a is the activation energy required for the reaction to occur (J/mol), R is the gas constant (8.314 J/Kmol), T is the reaction temperature ($^{\circ}\text{K}$), and A is the frequency factor. A semilogarithmic graphic of deposition rates versus different substrate temperatures is presented in Figure 3.

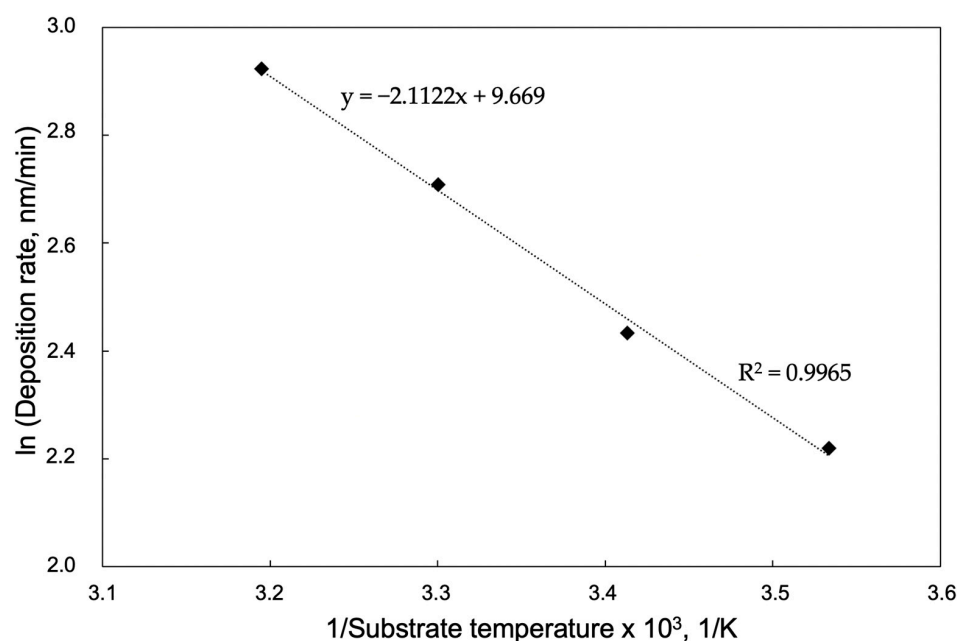


Figure 3. Semilogarithmic graphic of PDPAEMA deposition rates versus different substrate temperatures at a plasma power of 60 W and a reactor pressure of 300 mtorr.

If the surface reaction rate is lower than the adsorption rate, then the activation energy should be positive. In the opposite case, the activation energy is negative. From Figure 3, the activation energy of PDPAEMA was calculated as 17.56 kJ/mol. Since the reaction rate increases with increasing temperature, the activation value greater than zero is unsurprising.

3.2. Film Structures

The chemical structure of the PDPAEMA thin film deposited at the highest deposition rate was revealed. The comparison of the FTIR spectra of the PDPAEMA thin

film and the DPAEMA monomer is given in Figure 4a. Both spectra were thickness-normalized and baseline-corrected. The FTIR spectra of both the PDPAEMA and the DPAEMA monomer displayed the following major peak assignments: C-H vibrations (2960 , 2930 , and 2880 cm^{-1}), C=O bond (1730 cm^{-1}), C-H bending (1500 – 1350 cm^{-1}), C-N stretching vibration (1025 cm^{-1}) [36,37]. However, the C=C bond observed at 1650 cm^{-1} in the monomer spectrum was not observed in the spectrum of the PDPAEMA thin film. The absence of C=C bonds in the thin film indicates that the polymerization proceeded through C=C bonds without any entrained monomer in the as-produced polymer.

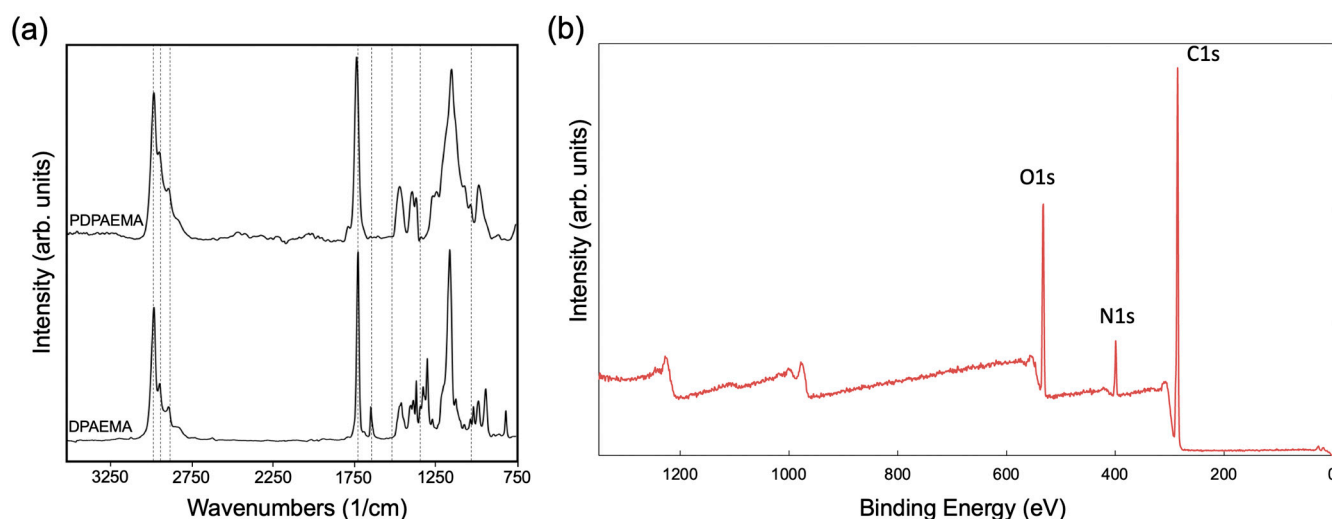


Figure 4. (a) FTIR spectra comparison of DPAEMA monomer and PDPAEMA, (b) XPS survey spectra of PDPAEMA.

Looking at the FTIR spectrum of PDPAEMA, it is important to note here that, unlike PDPAEMA produced using different methods, some peak broadening and peak intensity were observed in this study. This is unsurprising because in PECVD polymerizations intense bombardments of ions, electrons, neutrals, etc. may lead to a certain degree of functional group loss and extensive fragmentation of the polymer [38–40]. Furthermore, the chemical structure of the PDPAEMA thin film was confirmed by XPS analysis. As expected, only C, O, and N atoms were observed in the thin film in the XPS survey scan analysis (Figure 4b). The atomic percentages of C, O, and N elements were found to be 75.7, 17.5, and 6.8 at.%, respectively. These values are very close to the values calculated in the chemical structure of the DPAEMA monomer (79.2 at.% C, 13.2 at.% O, 6.6 at.% N). More detailed chemical investigation of the PDPAEMA thin film was carried out by the high-resolution mode of XPS. C1s spectrum of the PDPAEMA thin film can be curve-fitted into six components at binding energies of 289.1, 286.9, 286.1, 285.6, 285.1, and 284.7 eV, which can be attributed to $-\underline{\text{C}}=\text{O}$, $-\text{O}-\underline{\text{C}}\text{H}_2-$, $-\text{N}-\underline{\text{C}}\text{H}_2-$, $-\underline{\text{C}}-(\text{CH}_3)$, $-\underline{\text{C}}\text{H}-\text{N}-$, and $-\underline{\text{C}}\text{H}_3$, respectively (Figure 5a). O1s spectrum of the PDPAEMA thin film can be curve-fitted into two components at binding energies of 533.8 and 532.5 eV which can be attributed to $-\text{OCH}_3$ and $-\text{C}=\underline{\text{O}}$, respectively (Figure 5b) [41]. The large similarities in the main peaks between the FTIR spectra of the monomer DPAEMA and the PDPAEMA thin film indicate a high retention of the monomer structure. Furthermore, the chemical bonds observed in the high-resolution XPS analysis confirm that the PDPAEMA thin film was successfully synthesized.

In order to investigate the response of the PDPAEMA thin film to pH change, contact angles were measured after exposure to acidic and basic solutions. When PDPAEMA coated fabric was exposed to acidic solution, the fabric was completely wetted. After exposure to basic solution, PDPAEMA coated fabric showed hydrophobic behavior, and the contact angle value was measured as 114.7° . This dramatic change in the contact angle measurements is attributed to the ionizable tertiary amine group in the PDPAEMA

thin film, which is able to accept or donate protons according to the pH value of the solutions to which they are exposed [42]. From the studies in the literature, it is known that the pKa value of the PDPAEMA thin film is in the range of 6.5 to 6.8 [43,44]. In this study, when the pH value decreased to 3, tertiary amine groups were protonated and exhibited hydrophilic behavior due to the expansion of polymer chains with the effect of electrostatic repulsion force. When the pH value increased to 10, tertiary amine groups were deprotonated and the PDPAEMA thin film exhibited hydrophobic behavior as a result of aggregation of the polymer chains. Depending on the ambient pH, it is very important that the change in the contact angle of pH-responsive polymers is reversible. In order to display that the PDPAEMA thin film produced in this study has this capability, it was exposed to successively acidic and basic solutions. Figure 6a shows the contact angles of the PDPAEMA coated fabric after successive exposure to acidic and basic solutions, whereby similar contact angles were measured after each acid/base treatment cycle. Even after five repeated cycles, no significant change in the contact angle values was observed. Based on all these observations, it can be concluded that the thin film is chemically stable and the retention of functional groups of the monomer is high in the synthesized thin film. The predicted change in the chemical structure of the PDPAEMA thin film when exposed to acidic and basic solutions is presented in Figure 6b.

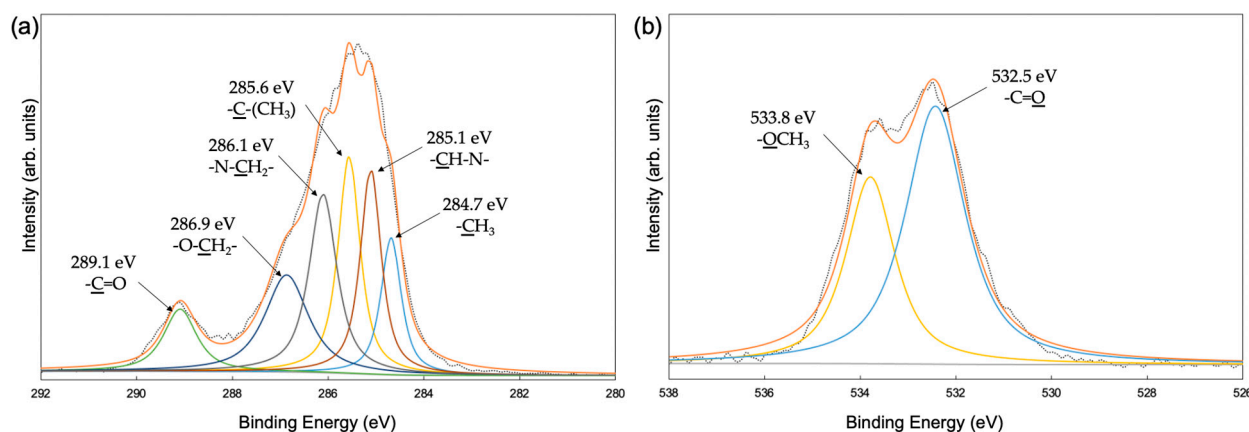


Figure 5. (a) Fitted C1s high resolution XPS spectrum of the PDPAEMA thin film. Green = $-\underline{\text{C}}=\text{O}$; dark blue = $-\text{O}-\underline{\text{C}}\text{H}_2$; grey = $-\text{N}-\underline{\text{C}}\text{H}_2-$; yellow = $-\underline{\text{C}}-(\text{CH}_3)$; red = $-\underline{\text{C}}\text{H}-\text{N}-$; light blue = $-\underline{\text{C}}\text{H}_3$, (b) Fitted O1s spectrum of the PDPAEMA thin film. Yellow = $-\text{O}\underline{\text{C}}\text{H}_3$; light blue = $-\text{C}=\underline{\text{O}}$. The raw curve and the fitted curve were shown in dotted and orange lines, respectively.

It is quite difficult to coat fragile substrates such as fabric using traditional wet polymerization methods. In this study, PDPAEMA thin film was successfully coated on fabric by the PECVD method due to its dry nature. SEM images of PDPAEMA coated and uncoated fabrics are shown in Figure 7a–d. No difference was observed between the appearance of both fabrics. The porous structure of the fabric is well preserved after coating, which indicates excellent conformal deposition.

PDPAEMA thin film produced by the PECVD method can be used in areas where the use of it when produced in bulk by conventional methods is very difficult or impossible. For example, PDPAEMA thin film produced at the nanoscale is expected to have high optical transmittance unlike the bulk polymer. The photographs of uncoated and PDPAEMA thin film coated glasses are shown in Figure 8a. No difference in the general appearance of the glasses was observed with the naked eye. The comparison of the optical transmittances of uncoated and PDPAEMA coated glasses is shown in Figure 8b. It can be seen that PDPAEMA thin film does not cause any significant absorption and optical loss in the visible range.

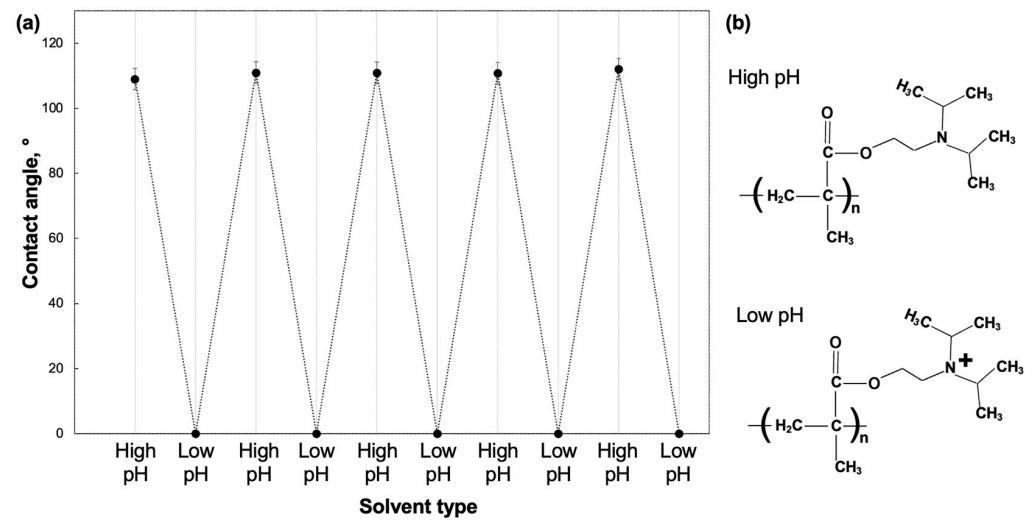


Figure 6. (a) The contact angle values of the PDPAEMA coated fabric as a function of repeated acid/base treatment cycles. (b) Reversible protonation/deprotonation process for the PDPAEMA thin film at high and low pH values.

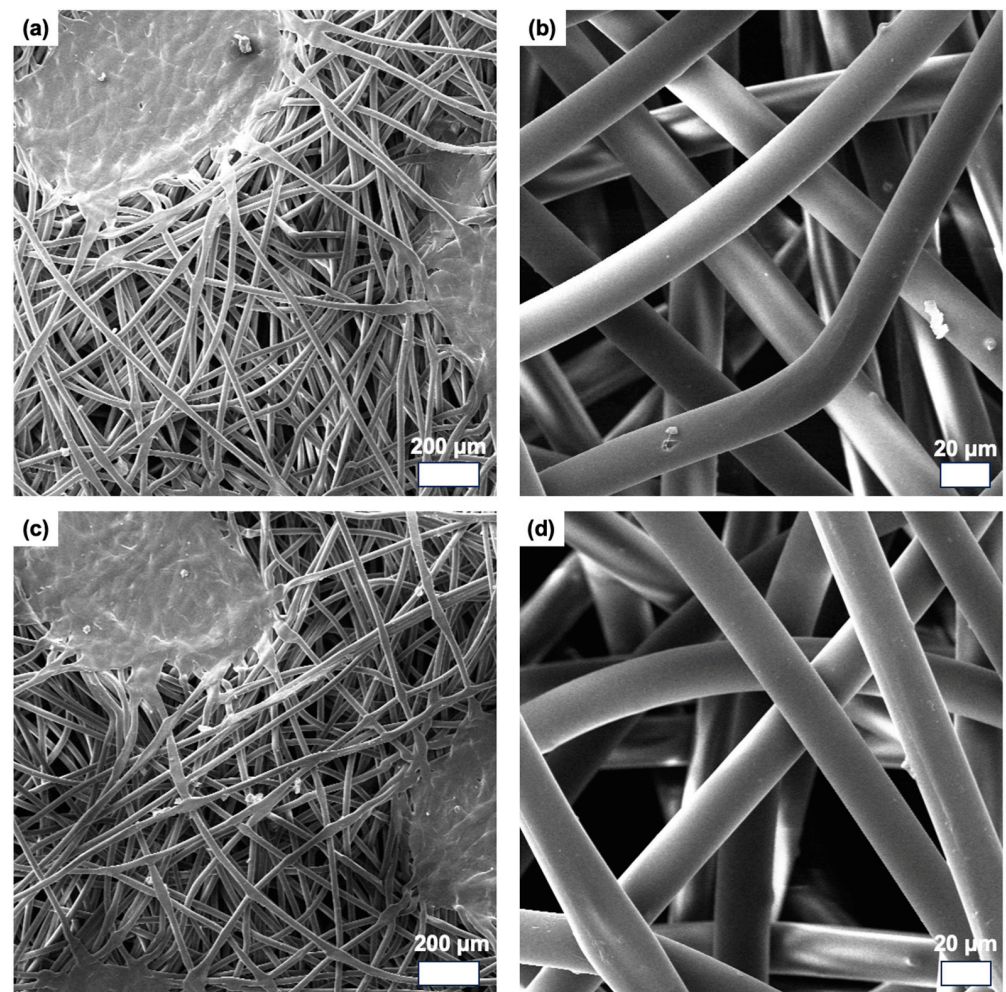


Figure 7. Low and high magnification SEM images of (a,b) uncoated and (c,d) PDPAEMA coated fabrics.

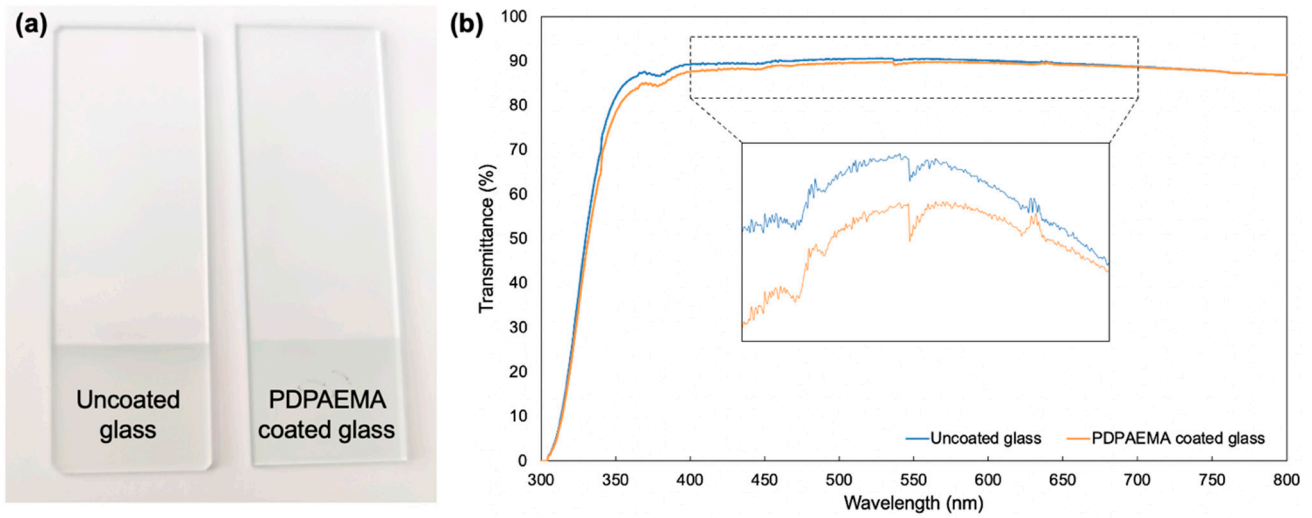


Figure 8. (a) The photographs and (b) the optical transmittances of uncoated and PDPAEMA coated glasses.

3.3. Large-Scale Deposition

Large area (16 cm diameter) thickness and roughness uniformities of the 10 min as-deposited PDPAEMA thin film were investigated. Fifteen silicon wafers were placed and coated on the reactor bottom as shown schematically in Figure 9. The reactor bottom was divided into three areas and five silicon wafers were placed in each area. In each area, the roughness value of one of the five silicon wafers and the film thicknesses of the other four were calculated. The measured thickness values were written regarding each silicon wafer as schematically shown in Figure 9. The average thickness value and standard deviation were found to be 186 nm and 5.6, respectively. Topographic images and roughness values of the films analyzed by AFM are shown next to their respective areas (Figure 9). The similar values and low standard deviations of both AFM and film thickness measurements indicate homogenous thin film coating in large scale. Furthermore, considering the easy integration of processes used for large-scale production such as roll-to-roll into CVD systems [45,46], it can be suggested that PDPAEMA thin film produced by the PECVD method has high potential for use in industrial applications.

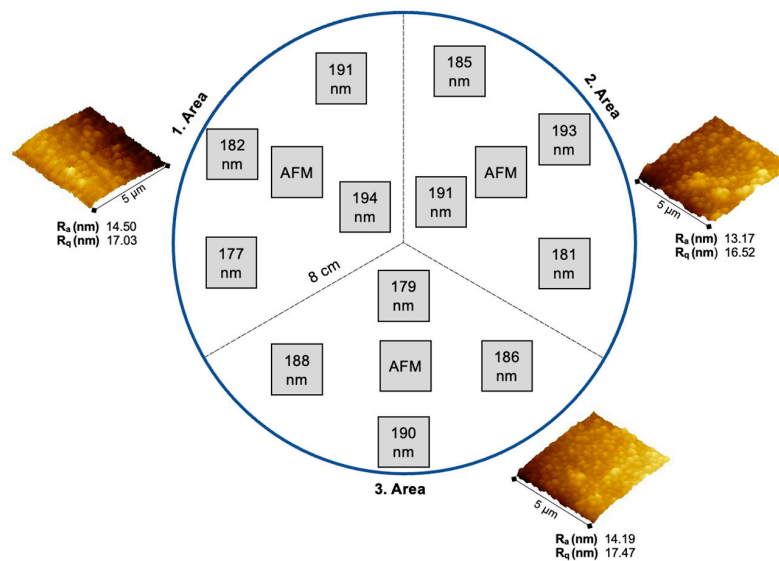


Figure 9. Schematic representation of silicon wafers placed on the reactor bottom with measured film thickness values and AFM results.

4. Conclusions

The highest deposition rate was found to be 18.6 nm/min at a substrate temperature of 40 °C, a reactor pressure of 300 mtorr, and a plasma power of 60 W. The deposition mechanism of PDPAEMA thin film was investigated. It was found that the rate-limiting step in the PECVD of PDPAEMA polymerization is surface reactions. The apparent activation energy was calculated to be 17.56 kJ/mol. It was observed that the wettability of the PDPAEMA thin film changes depending on the pH of the medium. PDPAEMA thin film showed high optical transmittance in the visible range and excellent conformal coverage. In large-scale synthesis, the similar surface roughness and film thickness values were measured. According to the results obtained in this study, PDPAEMA thin film produced by the PECVD method has the potential to be used in many areas where pH-responsive polymers are used. Moreover, the strategy developed here can be used to fabricate other functional thin films.

Funding: This study was supported by the Scientific and Technological Research Council of Turkey (TÜBİTAK) with a grant number of 119M227.

Institutional Review Board Statement: Not applicable.

Informed Consent Statement: Not applicable.

Data Availability Statement: Data are contained within the article.

Acknowledgments: The author thanks Emine Sevgili Mercan from Konya Technical University for fruitful discussion on the XPS analysis.

Conflicts of Interest: The author declares no conflict of interest.

References

1. Png, Z.M.; Wang, C.-G.; Yeo, J.; Lee, J.J.C.; Surat'man, N.E.B.; Tan, Y.L.; Liu, H.; Wang, P.; Tan, M.B.H.; Xu, J.; et al. Stimuli-responsive Structure-Property Switchable Polymer Materials. *Mol. Syst. Des. Eng.* **2023**, *8*, 1097–1129. [[CrossRef](#)]
2. Wurm, F.R.; Boyer, C.; Sumerlin, B.S. Progress on Stimuli-Responsive Polymers. *Macromol. Rapid Commun.* **2021**, *42*, 2100512. [[CrossRef](#)] [[PubMed](#)]
3. Gao, Y.; Wei, M.; Li, X.; Xu, W.; Ahiabu, A.; Perdiz, J.; Liu, Z.; Serpe, M.J. Stimuli-responsive polymers: Fundamental considerations and applications. *Macromol. Res.* **2017**, *25*, 513–527. [[CrossRef](#)]
4. Siniscalco, D.; Pessoni, L.; Boussonnière, A.; Castanet, A.-S.; Billon, L.; Vignaud, G.; Delorme, N. Design of an Azopolymer for Photo-Switchable Adhesive Applications. *Coatings* **2024**, *14*, 275. [[CrossRef](#)]
5. Guisasaola, E.; Baeza, A.; Talelli, M.; Arcos, D.; Moros, M.; de la Fuente, J.M.; Vallet-Regi, M. Magnetic-responsive release controlled by hot spot effect. *Langmuir* **2015**, *31*, 12777–12782. [[CrossRef](#)] [[PubMed](#)]
6. Stamou, A.; Iatrou, H.; Tsitsilianis, C. NIPAm-based modification of poly (L-lysine): A pH-dependent LCST-type thermo-responsive biodegradable polymer. *Polymers* **2022**, *14*, 802. [[CrossRef](#)] [[PubMed](#)]
7. Jing, H.; Huang, X.; Du, X.; Mo, L.; Ma, C.; Wang, H. Facile synthesis of pH-responsive sodium alginate/carboxymethyl chitosan hydrogel beads promoted by hydrogen bond. *Carbohydr. Polym.* **2022**, *278*, 118993. [[CrossRef](#)] [[PubMed](#)]
8. Yusa, S.-I. Development and application of pH-responsive polymers. *Polym. J.* **2022**, *54*, 235–242. [[CrossRef](#)]
9. Ofridam, F.; Tarhini, M.; Lebaz, N.; Gagnière, É.; Mangin, D.; Elaissari, A. pH-sensitive polymers: Classification and some fine potential applications. *Polym. Adv. Technol.* **2021**, *32*, 1455–1484. [[CrossRef](#)]
10. Kocak, G.; Tuncer, C.; Bütün, V. pH-Responsive polymers. *Polym. Chem.* **2017**, *8*, 144–176. [[CrossRef](#)]
11. Bazban-Shotorbani, S.; Hasani-Sadrabadi, M.M.; Karkhaneh, A.; Serpooshan, V.; Jacob, K.I.; Moshaverinia, A.; Mahmoudi, M. Revisiting structure-property relationship of pH-responsive polymers for drug delivery applications. *J. Control. Release* **2017**, *253*, 46–63. [[CrossRef](#)]
12. Wang, L.; Ren, K.-F.; Wang, H.-B.; Wang, Y.; Ji, J. pH-sensitive controlled release of doxorubicin from polyelectrolyte multilayers. *Colloids Surf. B Biointerfaces* **2015**, *125*, 127–133. [[CrossRef](#)] [[PubMed](#)]
13. Zhu, L.; Smith, P.P.; Boyes, S.G. pH-responsive polymers for imaging acidic biological environments in tumors. *J. Polym. Sci. Part B Polym. Phys.* **2013**, *51*, 1062–1067. [[CrossRef](#)]
14. Hu, J.; Zhang, G.; Ge, Z.; Liu, S. Stimuli-responsive tertiary amine methacrylate-based block copolymers: Synthesis, supramolecular self-assembly and functional applications. *Prog. Polym. Sci.* **2014**, *39*, 1096–1143. [[CrossRef](#)]
15. Gorji, M.; Zarbaf, D.; Mazinani, S.; Noushabadi, A.S.; Cella, M.A.; Sadeghianmaryan, A.; Ahmadi, A. Multi-responsive on-demand drug delivery PMMA-co-PDEAEMA platform based on CO₂, electric potential, and pH switchable nanofibrous membranes. *J. Biomater. Sci. Polym. Ed.* **2023**, *34*, 351–371. [[CrossRef](#)] [[PubMed](#)]

16. Eygeris, Y.; Ulery, N.; Zharov, I. pH-Responsive Membranes from Self-Assembly of Poly (2-(dimethylamino) ethyl methacrylate) Brush Silica Nanoparticles. *Langmuir* **2023**, *39*, 15792–15798. [[CrossRef](#)] [[PubMed](#)]
17. Kongkatigumjorn, N.; Smith, S.A.; Chen, M.; Fang, K.; Yang, S.; Gillies, E.R.; Johnston, A.P.; Such, G.K. Controlling endosomal escape using pH-responsive nanoparticles with tunable disassembly. *ACS Appl. Nano Mater.* **2018**, *1*, 3164–3173. [[CrossRef](#)]
18. Echalié, C.; Jebors, S.; Laconde, G.; Brunel, L.; Verdié, P.; Causse, L.; Bethry, A.; Legrand, B.; Van Den Berghe, H.; Garric, X. Sol-gel synthesis of collagen-inspired peptide hydrogel. *Mater. Today* **2017**, *20*, 59–66. [[CrossRef](#)]
19. Amano, M.; Uchiyama, M.; Satoh, K.; Kamigaito, M. Sulfur-Free Radical RAFT Polymerization of Methacrylates in Homogeneous Solution: Design of exo-Olefin Chain-Transfer Agents (R-CH₂C(=CH₂)Z). *Angew. Chem. Int. Ed.* **2022**, *61*, e202212633. [[CrossRef](#)]
20. Wu, X.; Wyman, I.; Zhang, G.; Lin, J.; Liu, Z.; Wang, Y.; Hu, H. Preparation of superamphiphobic polymer-based coatings via spray-and dip-coating strategies. *Prog. Org. Coat.* **2016**, *90*, 463–471. [[CrossRef](#)]
21. Yu, X.; Yang, W.; Yang, Y.; Wang, X.; Liu, X.; Zhou, F.; Zhao, Y. Subsurface-initiated atom transfer radical polymerization: Effect of graft layer thickness and surface morphology on antibiofouling properties against different foulants. *J. Mater. Sci.* **2020**, *55*, 14544–14557. [[CrossRef](#)]
22. Gosar, Ž.; Kovač, J.; Mozetič, M.; Primc, G.; Vesel, A.; Zaplotnik, R. Deposition of SiO_xCyHz protective coatings on polymer substrates in an industrial-scale PECVD reactor. *Coatings* **2019**, *9*, 234. [[CrossRef](#)]
23. Gürsoy, M.; Kocadayıoğulları, B. Environmentally Friendly Approach for the Plasma Surface Modification of Fabrics for Improved Fog Harvesting Performance. *Fibers Polym.* **2023**, *24*, 3557–3567. [[CrossRef](#)]
24. Karaman, M.; Gürsoy, M.; Ayköl, F.; Tosun, Z.; Kars, M.D.; Yildiz, H.B. Hydrophobic coating of surfaces by plasma polymerization in an RF plasma reactor with an outer planar electrode: Synthesis, characterization and biocompatibility. *Plasma Sci. Technol.* **2017**, *19*, 085503. [[CrossRef](#)]
25. Gürsoy, M.; Uçar, T.; Tosun, Z.; Karaman, M. Initiation of 2-hydroxyethyl methacrylate polymerization by tert-butyl peroxide in a planar PECVD system. *Plasma Process. Polym.* **2016**, *13*, 438–446. [[CrossRef](#)]
26. Saenger, K.; Tong, H. Laser interferometry: A measurement technique for diffusion studies in thin polymer films. *Polym. Eng. Sci.* **1991**, *31*, 432–435. [[CrossRef](#)]
27. Yasuda, H.; Wang, C. Plasma polymerization investigated by the substrate temperature dependence. *J. Polym. Sci. Polym. Chem. Ed.* **1985**, *23*, 87–106. [[CrossRef](#)]
28. d’Agostino, R.; Cramarossa, F.; Fracassi, F.; Illuzzi, F. Plasma polymerization of fluorocarbons. *Plasma Depos. Treat. Etch. Polym.* **1990**, *2*, 95–162.
29. Gürsoy, M.; Karaman, M. Improvement of wetting properties of expanded perlite particles by an organic conformal coating. *Prog. Org. Coat.* **2018**, *120*, 190–197. [[CrossRef](#)]
30. Wu, D.; Lo, W.; Chang, L.; Horng, R.-H. Properties of SiO₂-like barrier layers on polyethersulfone substrates by low-temperature plasma-enhanced chemical vapor deposition. *Thin Solid Films* **2004**, *468*, 105–108. [[CrossRef](#)]
31. Ozaydin-Ince, G.; Gleason, K.K. Transition between kinetic and mass transfer regimes in the initiated chemical vapor deposition from ethylene glycol diacrylate. *J. Vac. Sci. Technol. A* **2009**, *27*, 1135–1143. [[CrossRef](#)]
32. Mercan, E.S.; Karaman, M. Coating of hydrophilic poly (hydroxypropyl methacrylate) thin films via pulsed-initiated chemical vapor deposition method. *J. Coat. Technol. Res.* **2021**, *18*, 1261–1268. [[CrossRef](#)]
33. Karaman, M.; Gürsoy, M.; Kuş, M.; Özel, F.; Yenel, E.; Şahin, Ö.G.; Kivrak, H.D. Chemical and physical modification of surfaces. In *Surface Treatments for Biological, Chemical, and Physical Applications*; Wiley: Hoboken, NJ, USA, 2017; pp. 23–66.
34. Mao, Y.; Gleason, K.K. Hot filament chemical vapor deposition of poly (glycidyl methacrylate) thin films using tert-butyl peroxide as an initiator. *Langmuir* **2004**, *20*, 2484–2488. [[CrossRef](#)] [[PubMed](#)]
35. Martin, T.P.; Gleason, K.K. Combinatorial initiated CVD for polymeric thin films. *Chem. Vap. Depos.* **2006**, *12*, 685–691. [[CrossRef](#)]
36. Lin-Vien, D.; Colthup, N.B.; Fateley, W.G.; Grasselli, J.G. *The Handbook of Infrared and Raman Characteristic Frequencies of Organic Molecules*; Elsevier: Amsterdam, The Netherlands, 1991.
37. Günzler, H.; Gremlich, H.-U. *IR Spectroscopy. An Introduction*; IAEA: Vienna, Austria, 2002.
38. Gürsoy, M. Fabrication of paper-based microfluidic devices using PECVD for selective separation. *Macromol. Res.* **2021**, *29*, 423–429. [[CrossRef](#)]
39. Biederman, H.; Slavinská, D. Plasma polymer films and their future prospects. *Surf. Coat. Technol.* **2000**, *125*, 371–376. [[CrossRef](#)]
40. Rupper, P.; Vandenbossche, M.; Bernard, L.; Hegemann, D.; Heuberger, M. Composition and stability of plasma polymer films exhibiting vertical chemical gradients. *Langmuir* **2017**, *33*, 2340–2352. [[CrossRef](#)] [[PubMed](#)]
41. Beamson, G. *High Resolution XPS of Organic Polymers. The Scienta ESCA 300 Database. IC1plc*; Wiley: Chichester, UK, 1992.
42. Karaman, M.; Çabuk, N. Initiated chemical vapor deposition of pH responsive poly (2-diisopropylamino) ethyl methacrylate thin films. *Thin Solid Films* **2012**, *520*, 6484–6488. [[CrossRef](#)]
43. Fielding, L.A.; Edmondson, S.; Armes, S.P. Synthesis of pH-responsive tertiary amine methacrylate polymer brushes and their response to acidic vapour. *J. Mater. Chem.* **2011**, *21*, 11773–11780. [[CrossRef](#)]
44. Giacomelli, F.C.; Štěpánek, P.; Giacomelli, C.; Schmidt, V.; Jäger, E.; Jäger, A.; Ulbrich, K. pH-triggered block copolymer micelles based on a pH-responsive PDPA (poly [2-(diisopropylamino) ethyl methacrylate]) inner core and a PEO (poly (ethylene oxide)) outer shell as a potential tool for the cancer therapy. *Soft Matter* **2011**, *7*, 9316–9325. [[CrossRef](#)]

45. Cheng, C.; Gupta, M. Roll-to-roll surface modification of cellulose paper via initiated chemical vapor deposition. *Ind. Eng. Chem. Res.* **2018**, *57*, 11675–11680. [[CrossRef](#)]
46. Shrestha, S.; Parajuli, S.; Park, J.; Yang, H.; Cho, T.-Y.; Eom, J.-H.; Cho, S.-K.; Lim, J.; Cho, G.; Jung, Y. Improving Stability of Roll-to-Roll (R2R) Gravure-Printed Carbon Nanotube-Based Thin Film Transistors via R2R Plasma-Enhanced Chemical Vapor-Deposited Silicon Nitride. *Nanomaterials* **2023**, *13*, 559. [[CrossRef](#)] [[PubMed](#)]

Disclaimer/Publisher's Note: The statements, opinions and data contained in all publications are solely those of the individual author(s) and contributor(s) and not of MDPI and/or the editor(s). MDPI and/or the editor(s) disclaim responsibility for any injury to people or property resulting from any ideas, methods, instructions or products referred to in the content.